Atlantic Geology

Geochemistry and petrogenesis of the East Branch Brook metagabbroic dykes in the Sawyer Brook fault zone, Clarence Stream gold prospect, southwestern New Brunswick

Kathleen G. Thorne and David R. Lentz

Cite this article

Article abstract

The I:asi Branch Brook (F.BB) metagabbroic dykes, hosl to a portion of the Clarence Stream gold deposit, are situated within the contact tnelamorphic aureole of the Middle Devonian I-type Magaguadavic Granite on the northwestern margin ot the post-orogcnic Saint George Bathohth. They are highly deformed, light- (type I), intermediate- (type 2) to dark-coloured (type .1) dykes containing auriferous quart/ veins thai occupy brittle to ductile northeast-trending shear /ones in shallow marine, homfclsed. voleaniclastic. scdimcniary rocks of the Silurian Wawcig and Oak Bay formations The shear zones parallel the regional structure as a result of proximity to the faulted boundary (Sawyer Brook fault) between the Ordovician St. Croix terrane to the northwest and the Silurian to Karly Devonian Mascarenc Basin to the southeast. Geochemical studies of the FBB dykes indicate that three pulses (Fc-rieh. intermediate, and Mg-rich) of subalkalinc to slightly alkaline continental tholeiitc magmas were generated in a transprcssional environment dunng the Parly Silurian to liarly Devonian Positive t:v, values indicate their derivation from a partially depleted mantle source during faulting and nft-related events

Although the geochemical data (Fc- and Ti-depletion) indicate eale-alkaline affinity for the nearby Boeabcc intrusive complex, »,,, values and primitive mantle-normalized spider diagram patterns are similar to those of the FBB dykes In contrast, the St. Stephen Intrusion appears more primitive with wiihin-platc tholciitic to slightly alkalic affinity

Geochemistry and petrogenesis of the East Branch Brook metagabbroic dykes in the Sawyer Brook fault zone, Clarence Stream gold prospect, southwestern New Brunswick

Kathleen G. Thorne* and David R. Lentz
Department of Geology, University of New Brunswick, PO Box 4400, Fredericton, NB E3B 5A3
*Current address: New Brunswick Department of Natural Resources and Energy,
Geological Surveys Branch, P.O. Box 6000, Fredericton, NB E3B 5H1*
<kay.thorne@gnb.ca>

The East Branch Brook (EBB) metagabbroic dykes, host to a portion of the Clarence Stream gold deposit, are situated within the contact metamorphic aureole of the Middle Devonian I-type Magaguadavic Granite on the northwestern margin of the post-orogenic Saint George Batholith. They are highly deformed, light- (type 1), intermediate- (type 2) to dark-coloured (type 3) dykes containing auriferous quartz veins that occupy brittle to ductile northeast-trending shear zones in shallow marine, hornfelsed, volcaniclastic, sedimentary rocks of the Silurian Waweig and Oak Bay formations. The shear zones parallel the regional structure as a result of proximity to the faulted boundary (Sawyer Brook fault) between the Ordovician St. Croix terrane to the northwest and the Silurian to Early Devonian Mascarene Basin to the southeast. Geochemical studies of the EBB dykes indicate that three pulses (Fe-rich, intermediate, and Mg-rich) of subalkaline to slightly alkaline continental tholeiite magmas were generated in a transpressional environment during the Early Silurian to Early Devonian. Positive ε_{Nd} values indicate their derivation from a partially depleted mantle source during faulting and rift-related events.

Although the geochemical data (Fe- and Ti-depletion) indicate calc-alkaline affinity for the nearby Bocabec intrusive complex, ε_{Nd} values and primitive mantle-normalized spider diagram patterns are similar to those of the EBB dykes. In contrast, the St. Stephen Intrusion appears more primitive with within-plate tholeiitic to slightly alkalic affinity.

Les dykes métagabbroïques du ruisseau East Branch, qui abritent une partie du gîte aurifère de Clarence Stream, sont situées à l'intérieur de l'auréole de métamorphisme de contact du granite du Dévonien moyen de type I de Magaguadavic sur la limite nord-ouest du batholithe postorogénique de Saint George. Il s'agit de dykes extrêmement déformés de teinte pâle (type 1) et intermédiaire (type 2) à foncée (type 3) renfermant des filons de quartz aurifère qui occupent des zones de cisaillement cassantes à déformables, orientées vers le nord-est, dans des roches sédimentaires volcanoclastiques à cornéennes marines peu profondes des formations siluriennes de Waweig et d'Oak Bay. La proximité de la limite faillée (faille du ruisseau Sawyer) entre le terrane ordovicien de St. Croix, au nord-ouest, et le bassin du Silurien au Dévonien inférieur de Mascarene, au sud-est, a amené les zones du cisaillement à longer parallèlement la structure régionale. Des études géochimiques des dykes du ruisseau East Branch révèlent que trois impulsions (composante riche en fer, composante intermédiaire et composante riche en Mg) de magmas tholéiitiques continentaux, allant de subalcalins à légèrement alcalins, sont survenues dans un environnement transpressionnel pendant la période du Silurien inférieur au Dévonien inférieur. Les valeurs positives de ε_{Nd} témoignent de leur provenance d'un manteau partiellement appauvri pendant la formation de failles et des phénomènes apparentés à une distension.

Même si les données géochimiques (appauvrissement en Fe et en Ti) révèlent une affinité calcoalcaline du complexe intrusif proche de Bocabec, les valeurs de ε_{Nd} et les configurations de diagrammes en araignée normalisées du manteau primitif sont analogues à celles des dykes du ruisseau East Branch. Par contre, l'intrusion de Saint Stephen semble plus primitive avec une affinité intra-plaques allant de tholéiitique à légèrement alcaline.

Traduit par la rédaction

INTRODUCTION

The Clarence Stream gold deposit is situated in the Rollingdam area of southwestern New Brunswick (Fig. 1). It is within the contact metamorphic aureole of the magnetite-bearing, metaluminous, I-type Magaguadavic Granite (McLeod 1990), which comprises the northwestern portion of the Late Silurian to Late Devonian Saint George Batholith. A series of sheeted quartz veins occupy northeast-trending brittle to ductile shear zones, parallel to the intrusive contact with the batholith, and are locally the site of gold deposition (Thorne and Lentz 2001; Thorne et al. 2001). Also occupying a number of these shear zones are a series of gabbroic bodies that have experienced variable degrees of deformation, hydrothermal alteration, and metamorphism during regional orogenic and plutonic events. These mafic intrusions, referred to as the East Branch Brook (EBB) gabbro by the New Brunswick Department of Natural Resources and Energy
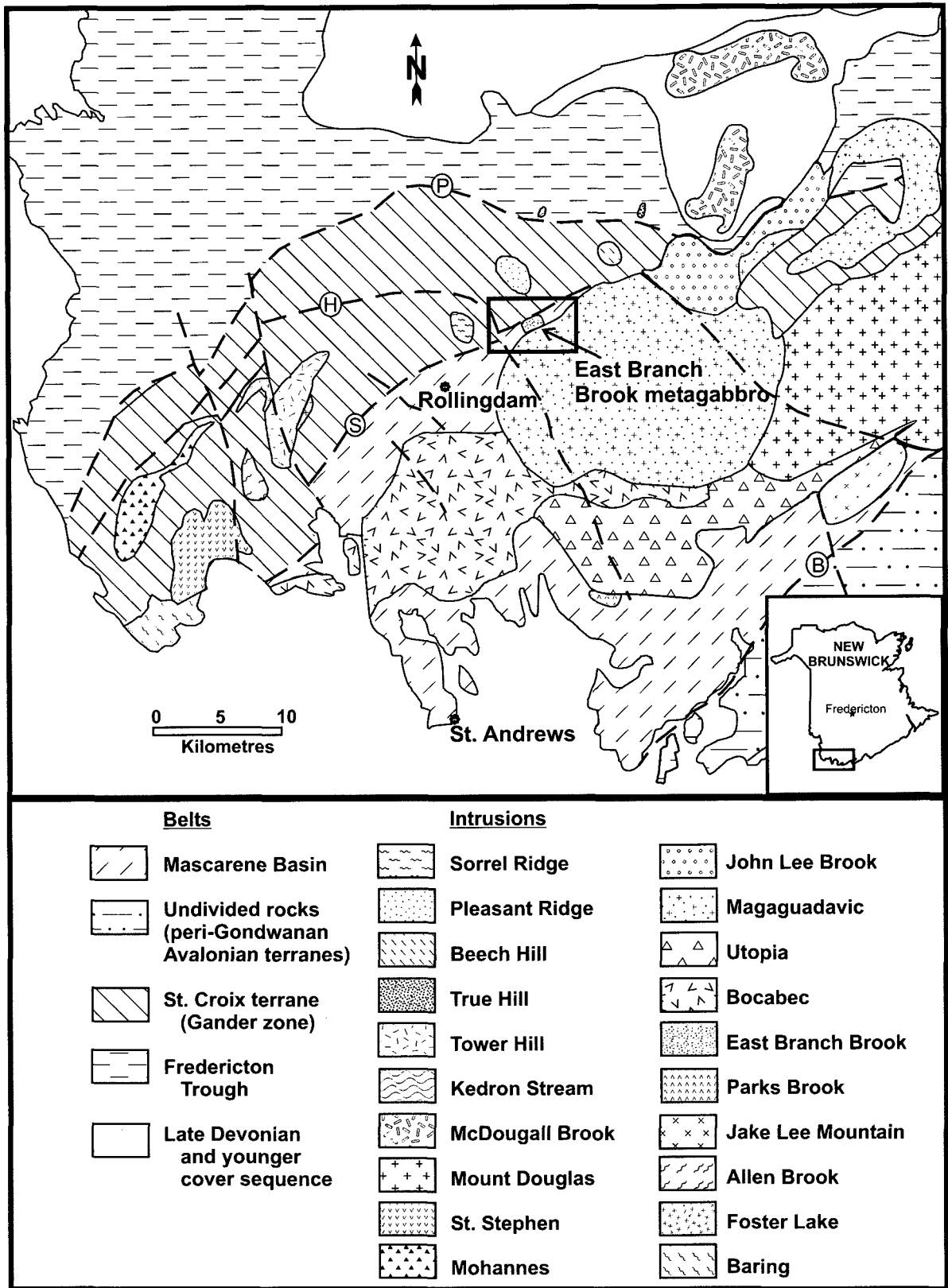
Fig. 1. Location map and regional geology of the Clarence Stream gold deposit in southwestern New Brunswick. Faults (represented by circled letters) include the Pendar Brook (P), Honeydale (H), Sawyer Brook (S), and Back Bay (B) faults. Geology compiled after McLeod (1990), McLeod *et al.* (1998), and New Brunswick Department of Natural Resources and Energy (2000).

(2000), are dykes hosted by Early to Late Silurian volcaniclastic metasedimentary units (L.R. Fyffe, personal communication, 2002), and therefore are no older than Silurian. Cross-cutting Devonian, auriferous, granitic pegmatite and aplite dykes (390 ± 8 Ma, U-Pb monazite; Thorne et al. 2002) genetically related to the late phase of the Magaguadavic Granite constrain their minimum age.

Relatively fresh samples from various intrusive phases of the EBB dykes were collected from trench exposures and outcrops immediately surrounding the Clarence Stream gold-bearing quartz vein system. We discuss the geochemistry, petrogenesis, and tectonic implications of these mafic units and compare them with re-analyzed samples of the Bocabec intrusive complex collected by Fyffe (1971). Fractionated samples taken from published data for the St. Stephen Intrusion (Paktunc 1989) were included as part of a more general comparison among mafic intrusions in the region.

REGIONAL GEOLOGY

The EBB metagabbroic dykes were emplaced near the suture zone between two major tectonostratigraphic terranes known as the St. Croix terrane of the Gander Zone to the northwest (Fig. 1; Fyffe and Fricker 1987), and the Late Neoproterozoic to Cambrian New River peri-Gondwanan terrane to the southeast (Fig. 1; Johnson and McLeod 1996; Fyffe et al. 1999), which was formerly interpreted as belonging to the Avalon Zone (Fyffe and Fricker 1987).

The St. Croix terrane is comprised of Ordovician clastic sedimentary rocks of the Cookson Group, which includes the Calais, Woodland, and Kendall Mountain formations, deposited as a continental slope sequence in an area of thinned continental crust (Ruitenberg et al. 1990; Fyffe and Riva 1990). Silurian turbidites of the Fredericton Trough flank the northwestern margin of the Ordovician St. Croix terrane (Fyffe and Fricker 1987). The syn- to post-sedimentary northeast-trending Sawyer Brook Fault bounds the St. Croix terrane to the south and juxtaposes back-arc basin sedimentary and volcanic sequences of the Silurian to Early Devonian Mascarene Group (Fyffe et al. 1999). The conglomeratic Oak Bay Formation, which marks the lower unit of the Silurian section in this area, contains clasts derived from the adjacent St. Croix terrane, and is overlain conformably by volcaniclastic and volcanic rocks of the Waweig Formation. The Mascarene Group units, and/or the bimodal intrusions of the Saint George Batholith and related intrusions to the southwest in New Brunswick and Maine, obscure the exact nature of the boundary between the St. Croix and New River terranes in the region (e.g., McLeod 1990; Whalen et al. 1996; Fyffe et al. 1999).

Numerous intrusions lie along the boundary between the Gander and Avalon zones (Fyffe and Fricker 1987), the largest being the bimodal plutonic rocks that comprise the Saint George Batholith (Fig. 1). The emplacement of these Late Silurian to Late Devonian magmas was strongly controlled by the orientation of the pre-existing NE-trending fault or terrane boundary (Cherry 1976). McLeod (1990) and Whalen et al. (1994) proposed that crustal melting generated the Saint George Batholith, initiated by underplating of mafic magma during transpressional movement along terrane boundaries.

The onset of plutonism within the Saint George Batholith was marked by nearly coeval mafic and felsic magmatism that produced the Bocabec intrusive complex, precise time of emplacement of which is not known. McLeod (1990) suggested a contemporaneous relationship between the Bocabec complex and the Utopia Granite, for which an $^{40}Ar/^{39}Ar$ age of 418 ± 5 Ma was obtained from biotite. A preliminary age of 430 ± 3 Ma (U-Pb zircon) has been reported for the Utopia Granite (Bevier 1990). However, this age is not consistent with the observed intrusive relationship with the Late Silurian volcanic rocks. More recent assessment of the U-Pb data revealed an average U-Pb age from 3 samples (2 zircon, 1 euxinite) of 423 ± 3 Ma (M.L. Bevier, personal communication, 2002), thus implying that a younger date in the range of 418 to 423 Ma is more appropriate. Fyffe (1971) described two types of diorite in the Bocabec complex, diabasic diorite with higher amounts of quartz, alkali feldspar, clinopyroxene, and opaque minerals and ophitic diorite that contains greater proportions of plagioclase, amphibole, biotite, and chlorite.

Ordovician sedimentary rocks belonging to the Cookson Group of the St. Croix terrane are host to the St. Stephen Intrusion, in which mafic and ultramafic rocks are well known for their nickel-copper deposits (Paktunc 1986, 1987, 1989). A conventional K-Ar hornblende age of 415 ± 19 Ma (Wanless et al. 1973) was obtained for this intrusion, the same time range as the Bocabec intrusive complex. More recent dating of phlogopite by $^{40}Ar/^{39}Ar$ yielded an age of 421 ± 5 Ma (S. Barr, personal communication, 2002).

The St. Stephen Intrusion is a tholeiitic intrusion comprised of various mafic-ultramafic units that include peridotite, troctolite, anorthosite, gabbro, and norite (Paktunc 1986, 1989). Olivine is a cumulus mineral in these units whereas plagioclase, clinopyroxene, and orthopyroxene are intercumulus minerals (Paktunc 1987). Together they comprise the dominant minerals of the five units although minor amounts of chromite, sulphide minerals, and ilmenite are also present (Paktunc 1987).

FIELD DESCRIPTION

An induced polarization geophysical survey of the Clarence Stream property revealed that the East Branch Brook intrusions are discrete linear features that span at least the length of the surveyed area (2.5 km) and trend toward the northeast. They occur in a highly strained area within the contact metamorphic aureole on the northwestern margin of the Magaguadavic Granite (Fig. 1). Dyke widths of up to 100 m are inferred from geophysical data as well as exposures in trenches excavated during various stages of gold exploration by Freewest Resources Canada Incorporated (Thorne and Lentz 2001; Thorne et al. 2001). They occupy and/or parallel vertical to steep north-dipping, brittle to ductile shear zones, which were subsequently reactivated and sealed by auriferous quartz veins. The overall trend of the gabbro bodies parallels the intrusive contact with the Magaguadavic Granite and is consistent with regional structure implying strong structural control on their emplacement. Rafts and screens of sheared sedimentary material form large xenoliths within the intrusive bodies. The dykes have experienced variable degrees of
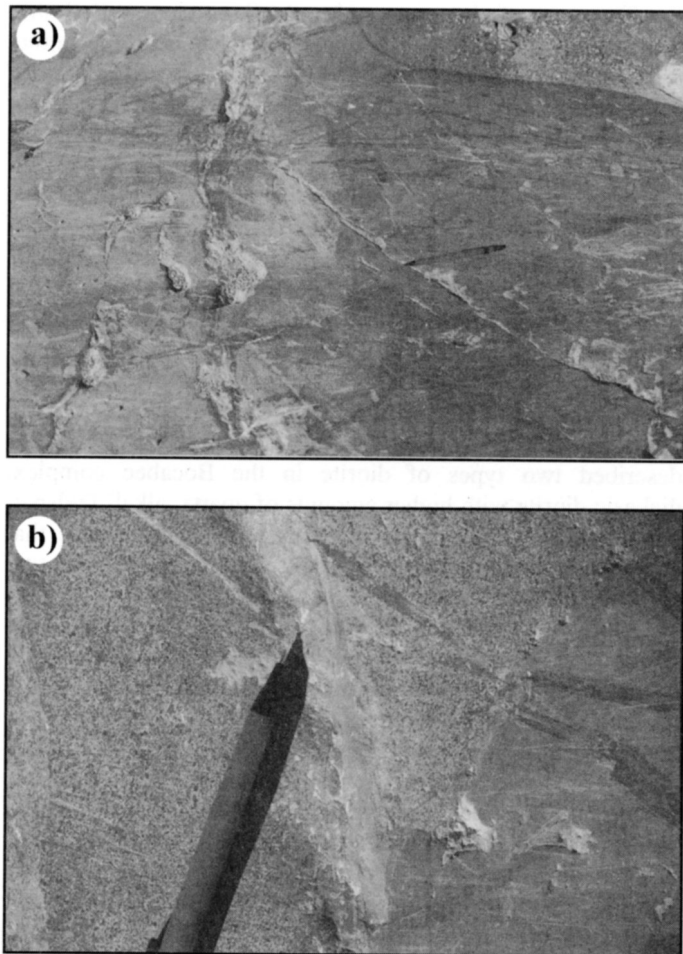
Fig. 2. Photographs of chilled margins between two metagabbroic bodies. In (a), the younger, dark green body (type 3) on the right intruded the older unit (type 1) on the left. In (b), small protruding dykelets confirm the relationship between the two units. Pencil length is 13 cm.
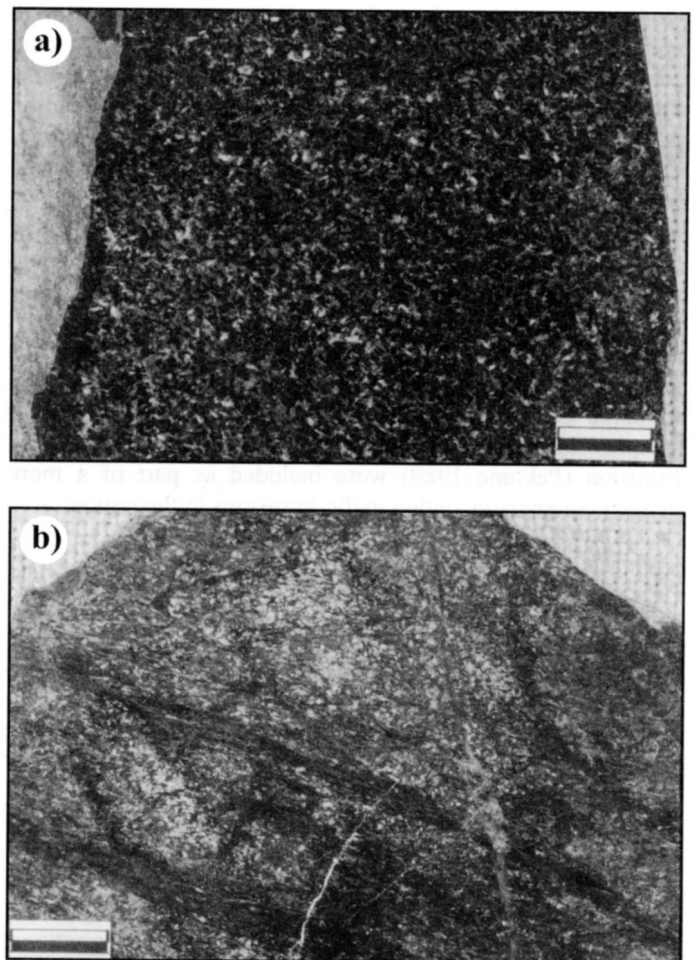

Fig. 3. Photographs of polished slabs exhibiting the textural variation related to shearing in the East Branch Brook metagabbro. a) Sample KM-00-22 (type 3) has a fresh, mottled texture. b) A distinct foliation is visible in sample KM-00-23 (type 3), which has darker chlorite-rich vein selveges surrounding lighter albite-rich zones that are cross-cut by small prehnite veinlets.

metamorphism, as described below, and hence are termed metagabbro.

Multiple intrusions of light-coloured to dark-coloured metagabbro comprise the EBB dykes. Colour variations of the dykes range from light grey-green to dark grey-green, and grain size ranges from fine to medium. In the field, these intrusions can be subdivided into three types based on the colour of their weathered surfaces [i.e. light (type 1), intermediate (type 2), and dark (type 3)]. This classification proved to be useful in defining three separate pulses of magmatism. The presence of chilled margins indicates that the lighter type is older than the darker type (Fig. 2). However, due to lack of exposure, their relationship with the intermediate (type 2) dykes is not discernible. It is assumed herein that the intermediate (type 2) dykes intruded after the light dykes and before the dark dykes. The dykes exhibit textural variation ranging from a fresh mottled texture typical in the less strained areas (Fig. 3a) to highly foliated (Fig. 3b) where shearing is evident.

The metagabbroic dykes contain variable amounts of disseminated oxides and sulphides such as magnetite (most common), pyrrhotite, pyrite, arsenopyrite, and stibnite that produce a highly iron-stained alteration with rare white arsenic

blooms where subjected to weathering. Subsequent felsic igneous activity in the Saint George Batholith also contributed to the alteration and metamorphism of the gabbro bodies, including amphibolitization, biotitization, albitization, and saussuritization. The intensity of biotitization varies dramatically and, where present, the outcrop exhibits a distinct purple hue. Albitization and saussuritization are most pervasive within the type 1 gabbros, with albite being the dominant mineral in the foliated matrix defined by variable amounts of muscovite and biotite. Clinopyroxene is replaced by light brown hornblende and actinolite, and relict primary plagioclase crystals are rare. Randomly oriented subhedral plagioclase and patchy biotite in a matrix of blue-green clinopyroxene partially altered to light brown amphibole (hornblende-actinolite) are typical of the type 2 and type 3 metagabbro dykes. The lighter colour of the weathered surface of the type 1 dykes may be attributed to pervasive amphibolitization of the pyroxene crystals whereas the younger dykes (types 2 and 3) show a lesser degree of metamorphism and hence better preservation of primary pyroxene crystals.

In areas of moderate to extreme deformation related to

shear zones, a well-preserved foliation defined by a biotite-muscovite-amphibole mineral assemblage can be distinguished in the dykes, which is subparallel to local bedding. A mineral defined down-dip lineation is also recognizable locally and reflects the latest dip-slip movement of the major shear system (A. Park, personal communication, 2002). High-temperature hydrothermal alteration is pervasive in these units, thus contributing to their extreme variability in fabric and colour.

MAJOR AND TRACE ELEMENT GEOCHEMISTRY

Analytical methods

Nineteen least-altered samples of the EBB metagabbroic dykes were collected from various trenches that were excavated during exploration activities on the Clarence Stream gold prospect in the Rollingdam area of southwestern New Brunswick (Fig. 1). Sample locations are documented in Table 1. Only samples that appeared to be relatively fresh were chosen in order to determine, as accurately as possible, their original composition. Weathered edges were carefully removed during sample collection. Crushing and pulverizing of nine samples were performed at Activation Laboratories Limited (Ancaster, Ontario) using mild (soft) steel apparatus, thus potentially contaminating the samples slightly with iron (up to 0.2%). A tungsten-carbide crusher was used to crush the remaining 10 samples at the University of New Brunswick, followed by pulverization using a mild steel swing mill.

The sample pulps were sent for Inductively Coupled Plasma-Emission Spectroscopy (ICP-ES), Inductively Coupled Plasma-Mass Spectroscopy (ICP-MS), and Instrumental Neutron Activation Analysis (INAA) at Activation Laboratories Limited (Ancaster, Ontario) to determine their trace-element content. X-ray Fluorescence Spectroscopy (XRF) of fused discs was performed at the University of Ottawa to analyze the major elements and selected trace elements. For comparison, selected mafic samples (9) from the Bocabec intrusive complex taken from the thesis collection of Fyffe (1971) were also sent for similar analysis. A gabbro standard (GB-1) (Lentz 1995) was used to quantify the error involved with each analytical procedure.

Upon comparison of the gabbro standard from this study with the accepted chemical composition of the standard, the percent errors for the sample suite were found to be as follows: <1%: MgO, Na$_2$O, Au, Ce, Tb, Be, In, W; <3%: SiO$_2$, Al$_2$O$_3$, Fe$_2$O$_3$, Nb, Hf, Lu, Ba; <5%: MnO, CaO, Ga, Yb; <10%: TiO$_2$, P$_2$O$_5$, Y, Co, Cr, Th, Sm, Sr; <15%: K$_2$O, Zr, Sc, La, Nd, Eu, Mo, V; <25%: Rb, Ta, Cu, Bi; >25%: Ni, Zn, U, Sb, Pb, Cd, Sn, As, Se, Ag, Cs, Tl, and Br. Analytical errors associated with the elements S, Re, Pr, Ho, Tm, Te, Li, Gd, and Er are unknown due to insufficient analyses of the standards.

Results

Table 2 contains average compositions for the three types of EBB dykes as well as the Bocabec and St. Stephen intrusions. Analytical data (major and trace elements) for the EBB metagabbroic samples are listed in Appendix 1. Major-

Table 1. Location of samples taken for analysis.

Sample*	Grid Coordinates[§]		UTM Coordinates (19T)	
	Easting	Northing	Easting	Northing
18	5+06E	0+82N	658025	5023473
19	4+90E	0+77N	658009	5023455
20	5+55E	0+75.15N	658067	5023486
21	5+54.75E	0+77.15N	658065	5023490
22	5+55.5E	0+84.2N	658063	5023496
23	4+97E	0+21.5N	658052	5023419
24	6+60.15E	0+22N	658210	5023461
25	8+58.5E	0+61.5N	658329	5023648
26	8+58.5E	0+70.5N	658329	5023648
113	20+02E	0+15S	659350	5024174
145	21+91E	0+24S	659511	5024279
146	22+04E	0+36.5S	659530	5024279
150	20+50E	1+30S	659447	5024083
155	18+78.5E	0+00BL	659232	5024122
156	16+54E	0+11.5N	659033	5024013
157	17+50E	0+00BL	659129	5024060
158	9+28E	0+00BL	658434	5023630
159	9+60E	0+02S	658454	5023638
160	6+08E	3+25S	658318	5023181

*Sample numbers preceded by KM-00-. [§]Coordinates are based on a cut grid used for exploration by Freewest Resources Canada Incorporated (Hoy 2001).

element chemistry indicates that the EBB metagabbroic samples are subalkalic to slightly alkalic gabbro based on the SiO$_2$ versus Na$_2$O+K$_2$O plot (TAS) designed for plutonic rocks (Fig. 4). The Bocabec samples in addition to the average sample from the St. Stephen Intrusion lie entirely within the subalkaline field (Fig. 4). Samples from the Bocabec intrusive complex labelled ophitic diorite by Fyffe (1971) plot within the gabbro field and the diabasic diorite samples are transitional between the gabbro and diorite field (Fig. 4). The majority of the EBB samples plot in the unaltered basalt field on the Na$_2$O–CaO diagram (Fig. 5), and hence major-element mobility is assumed to not have been sufficient to affect the classification of these samples, although some minor K addition (biotitization), pushes them into the alkaline TAS field (Fig. 4). Variation diagrams reveal that the EBB metagabbro samples are best described as low silica (46.83–51.15 wt %), high iron (Fe$_2$O$_3$[T]/MgO from 1.04 to 3.49 with an average value of 2.15) mafic intrusions that have high Na$_2$O (1.99–4.16 wt %) and CaO (7.63–10.93 wt %) contents (Fig. 6).

It is possible to categorize the dykes into three separate types with differing geochemical attributes that correspond closely to the light, intermediate, and dark classification applied to these samples in the field. The light-coloured metagabbro samples (type 1) tend to be enriched in Al$_2$O$_3$, CaO, MgO, and Cr with respect to the other samples, whereas the dark samples contain relatively equal or greater amounts of Fe$_2$O$_3$[T], Na$_2$O, and especially TiO$_2$ (up to 4.18 wt.%). The intermediate metagabbro samples are generally transitional between the other two types. Fig. 6f illustrates the path

followed by the three separate magmas related to their MgO and Cr compositional differences, with the earliest dykes being magnesium- and chrome-enriched with respect to the later dykes. The youngest intrusions (type 3) appear to be more evolved relative to the other types as they are titanium-enriched (Fig. 6e) thus coinciding with the observed crosscutting field relationships (Fig. 2). The Bocabec suite does not exhibit this TiO_2 enrichment and tends to closely resemble the more primitive early phase (type 1) of the EBB intrusions. The AFM ternary plot reveals that the majority of the EBB metagabbro samples are tholeiitic whereas the Bocabec samples appear to have calc-alkaline affinity (Fig. 7). However, this calc-alkaline signature may be a result of Na-metasomatism as the diabasic diorite samples lie outside the normal unaltered basalt field (Fig. 5). The type 1 metagabbro samples are relatively MgO-enriched and plot in the general vicinity of the Bocabec samples near the transition boundary between the tholeiitic and calc-alkaline fields. The field representing the St. Stephen Intrusion indicates that it is also tholeiitic, based on this diagram.

Discrimination plots that employ essentially immobile elements to determine the origin of magmatic suites are particularly useful when classifying the EBB metagabbroic samples due to the potential effects of alteration and metamorphic processes on sample geochemistry. Using Zr/TiO_2-Nb/Y ratios, the EBB metagabbroic samples tend to plot primarily in the andesite/basalt to subalkaline basalt field (Fig. 8), whereas the Bocabec samples exhibit a greater range with samples occupying the andesite, andesite/basalt, and subalkaline basalt fields. The Nb/Y ratios (Fig. 8) for the EBB metagabbros are consistent with subalkaline magmas, ranging from 0.18 to 0.46, as are those belonging to the Bocabec Complex with Nb/Y ratios in the range of 0.29 to 0.43. The average Nb/Y ratio for the St. Stephen suite is in the range of 0.73, just inside the alkalic field.

The EBB samples occupy the field between Ti/V ratios of 20 and 50 (Fig. 9). Type 1 metagabbroic samples tend to cluster closest to the origin (more primitive), whereas the two later types have greater proportions of Ti and V (Fig. 9). Although type 1 samples occupy the mid-ocean-ridge basalt/back-arc basin field, the type 2 and 3 samples follow a rift-related trend towards the continental flood basalt field. The Bocabec samples plot in the same area as the type 1 samples of the EBB intrusions, whereas the range of values obtained for the St. Stephen samples span all three tectonic environments (calc-alkaline and mid-ocean-ridge, or back-arc-basin fields). The St. Stephen Intrusion magmas appear to be more primitive in terms of their Ti and V contents than the type 1 EBB metagabbro and the Bocabec diorite/gabbro.

Using the Nb–Zr–Y plot (Fig. 10), the majority of the EBB metagabbroic samples plot in the field that encompasses within-plate tholeiite/volcanic-arc basalt, whereas one sample lies in the within-plate tholeiite field. Mafic samples from the Bocabec intrusive complex also plot in the same field as the EBB samples, although one sample (diabasic diorite) falls in the E-MORB field. A further distinction between the two environments is not possible by means of this diagram alone. Other data, such as geochemical plots and field relations, must be taken into account when assigning these magmas to their

Table 2. Average compositions of metagabbroic samples from the East Branch Brook intrusions, and Bocabec and St. Stephen complexes.

	Type 1	Type 2	Type 3	Bocabec[§]	St. Stephen*
Major elements (wt%)					
SiO_2	49.1	49.4	48.3	52.2	45.8
TiO_2	1.20	2.70	3.47	1.53	0.78
Al_2O_3	16.08	13.91	13.84	15.52	18.34
$Fe_2O_3{}^T$	10.20	11.38	14.64	10.49	8.89
MnO	0.19	0.23	0.24	0.19	0.15
MgO	8.21	5.38	4.52	5.44	11.90
CaO	8.38	8.76	8.85	8.05	9.13
Na_2O	2.50	3.51	3.48	3.31	1.94
K_2O	0.70	0.47	0.69	1.09	0.22
P_2O_5	0.20	0.34	0.44	0.24	0.14
LOI	1.48	1.08	1.20	–	2.38
Total	96.8	96.1	98.4	98.1	99.7
S	0.69	0.65	0.77	–	–
Mg#	61.2	43.7	38.1	50.0	–
Trace elements (in ppm, except Au in ppb)					
Cr	284	65	37	107	322
Ni	91	23	22	60	204
Co	37	25	34	46	50
Sc	35	45	43	–	–
V	247	391	504	217	13
Cu	27	20	68	–	58
Pb	19	61	143	3	12
Zn	112	119	133	124	89
Bi	0.07	0.19	0.24	–	–
Cd	0.40	0.36	0.70	–	–
Sn	0.4	1.0	1.0	–	–
Mo	14	32	29	–	–
As	120	59	249	–	15
Se	0.22	0.76	0.84	–	–
Sb	81	7	61	–	–
Te	0.04	0.10	0.04	–	–
Au	47	3	53	–	–
Rb	39	25	41	43	2
Cs	8.2	0.8	3.4	–	–
Ba	255	146	205	204	51
Sr	500	349	300	238	292
Tl	0.3	0.2	0.2	–	–
Ga	16	16	21	18	–
Li	24	19	5	–	–
Ta	0.41	0.25	0.55	–	–
Nb	6	10	13	15	6
Zr	111	183	221	183	31
Hf	3	4	6	–	–
Y	20	32	43	44	8
La	17.1	12.6	16.9	16.0	14.6
Th	3.1	1.7	2.3	5.9	–
U	0.6	0.4	0.5	–	–
Ce	40	27	48	54	–
Pr	3.5	4.5	2.1	–	–
Nd	18	24	25	39	–
Sm	4.3	5.0	6.6	–	–
Eu	1.4	1.8	2.6	–	–
Gd	2.0	4.4	2.0	–	–
Tb	0.54	1.16	1.06	–	–
Dy	1.7	4.7	2.2	–	–
Ho	0.4	1.1	0.5	–	–
Er	0.9	2.6	1.2	–	–
Tm	0.13	0.40	0.18	–	–
Yb	2.5	3.7	4.9	–	1.35
Lu	0.39	0.57	0.74	–	–
Br	0.25	0.25	0.25	–	–
Be	0.6	1.3	1.4	–	–

Notes: Type 1 (light), type 2 (intermediate) and type 3 (dark). * Data of Paktunc (1986). § Samples reanalysed from Fyffe (1971)
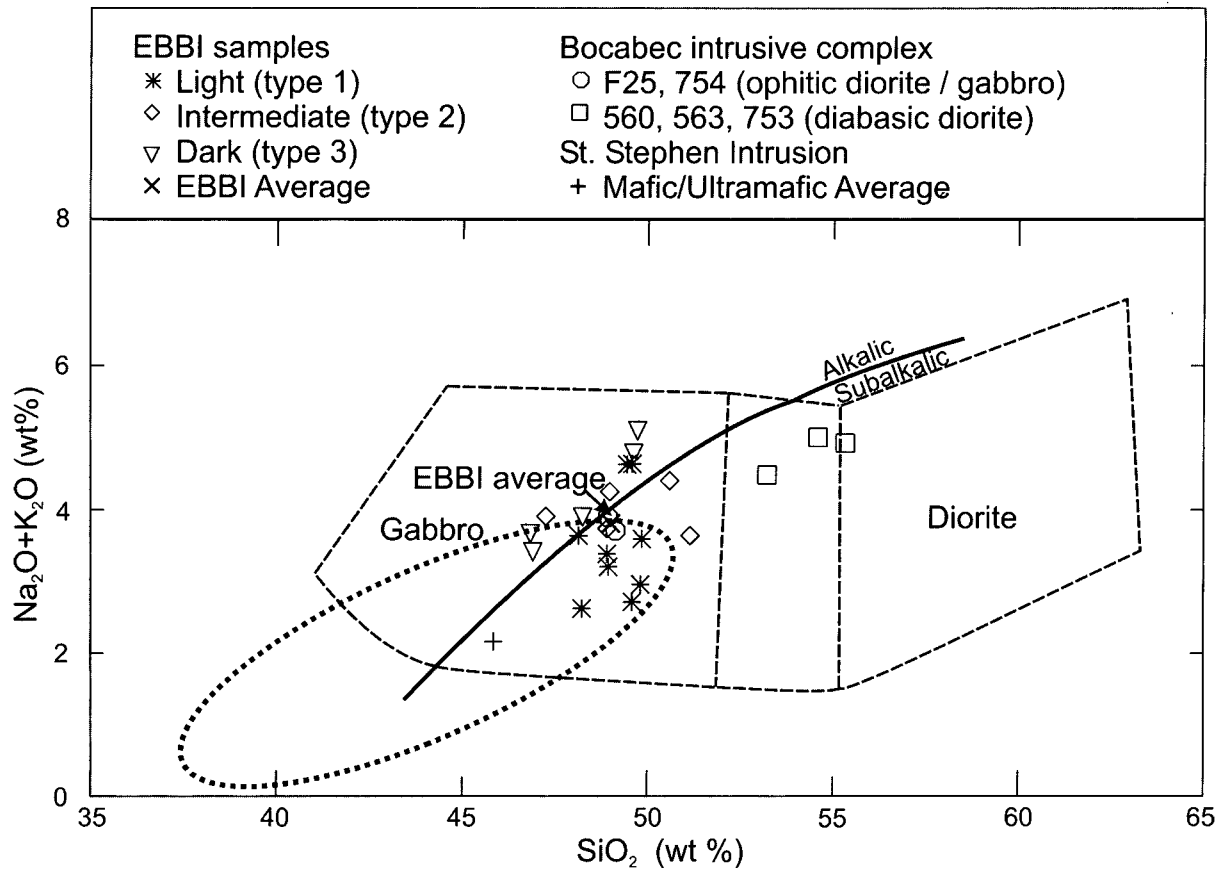
Fig. 4. Part of a total alkali (Na_2O + K_2O) versus silica diagram taken from Wilson (1989) as adapted from Cox *et al.* (1979) showing the gabbro and diorite fields. The solid line separates the alkalic field from the subalkalic field (Irvine and Baragar 1971). The field outlined by dashes includes 15 samples from the St. Stephen Intrusion (Paktunc 1989). Note that the East Branch Brook intrusions are represented by EBBI.

Fig. 5. Na_2O–CaO diagram showing the Na spilite, normal basalt, and normal unaltered basalt fields (after Graham 1976; Stillman and Williams 1979; Stephens 1982). Symbols are as in Fig. 4.

Fig. 6. MgO versus a) Al_2O_3, b) CaO, c) $Fe_2O_3^t$, d) Na_2O, e) TiO_2, and f) Cr illustrating the geochemical relationship between various intrusive units in relation to other mafic intrusions in the region. The dashed line represents the compositional evolution w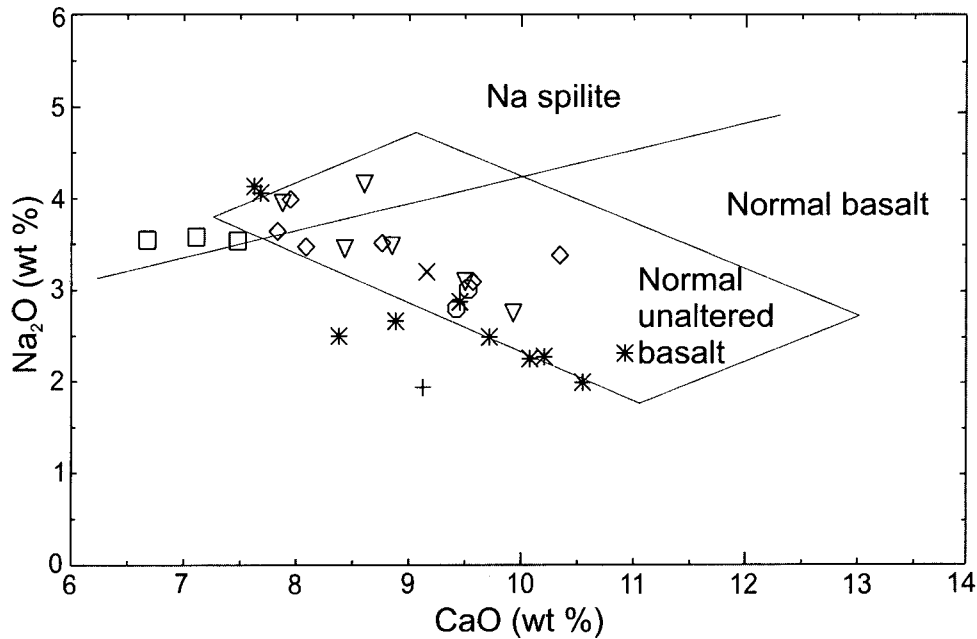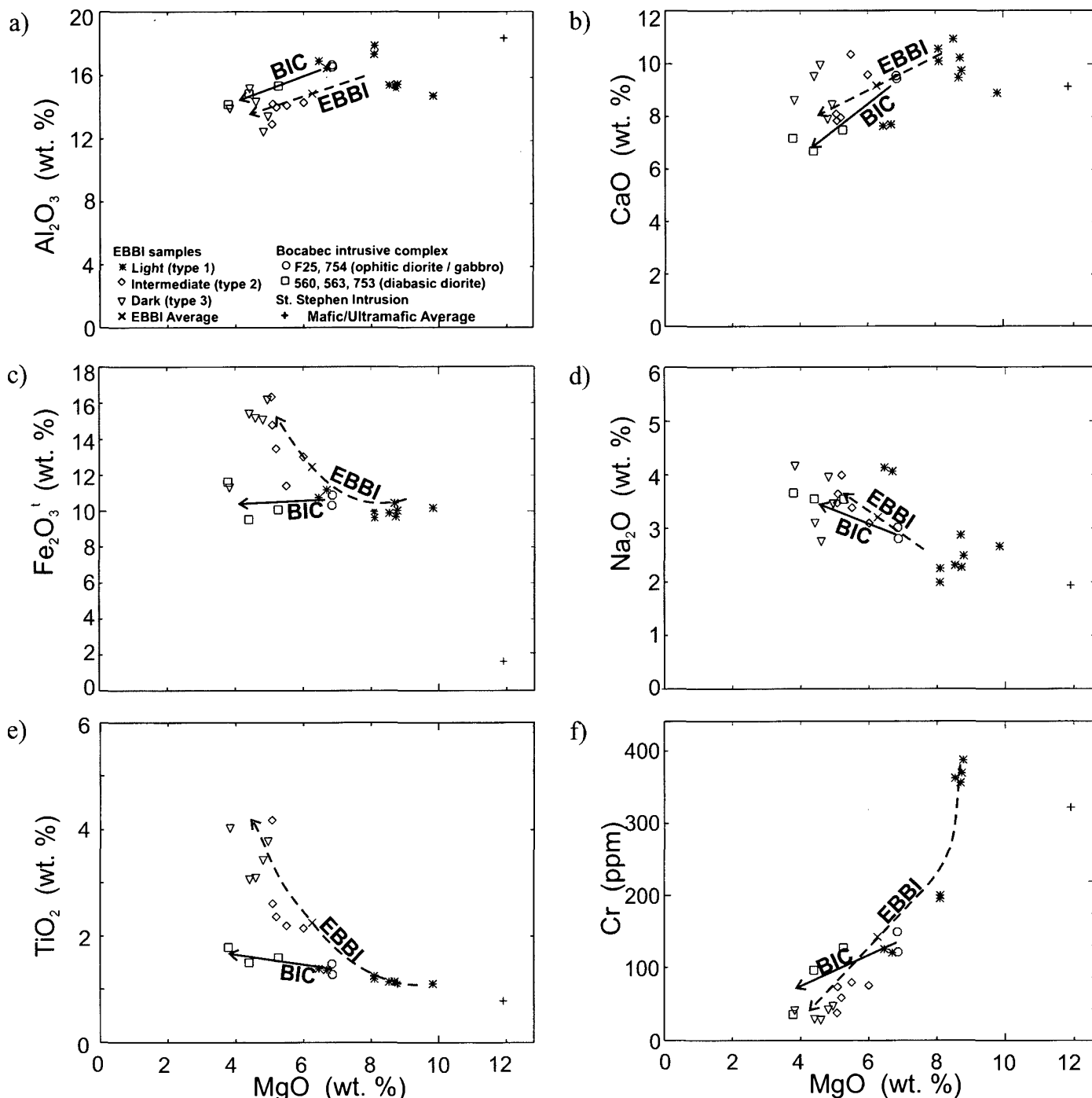hereas the solid line indicates an interpreted fractionation array. Symbols are as in Fig. 4. BIC- Bocabec intrusive complex, EBBI- East Branch Brook intrusions.

respective tectonic environments. The field of the mafic and ultramafic units of the St. Stephen intrusion lies primarily in the within-plate alkalic basalt/within-plate tholeiite field with overlap into the enriched MORB field (Fig. 10).

An overall enrichment in Large Ion Lithophile (LIL) elements (Cs, Rb, Ba, and K) is evident in the EBB samples relative to E-MORB and N-MORB (Fig. 11a). This trend is also seen in the Bocabec samples (Fig. 11b). The type 1 metagabbro is enriched in LIL elements over the subsequent intrusions, which may be explained in terms of crustal assimilation during the initial injection or possibly an

alteration effect. A slight light REE enrichment (La, Ce, Nd and Sm) is evident for both the EBB and Bocabec intrusions normalized against primitive mantle values (Fig. 11a and b). The Sr, Hf, Zr, and heavy REE contents of the EBB metagabbros are higher than that of N-MORB and E-MORB and plot closer to OIB (Fig. 11a). The type 1 dykes resemble the ophitic diorite samples of the Bocabec intrusive complex with their obvious and pronounced negative Nb anomalies possibly indicating crustal contamination (Fig. 11b). Spider diagram patterns for types 2 and 3 EBB dykes are quite similar, although type 3 is comparatively enriched in heavy
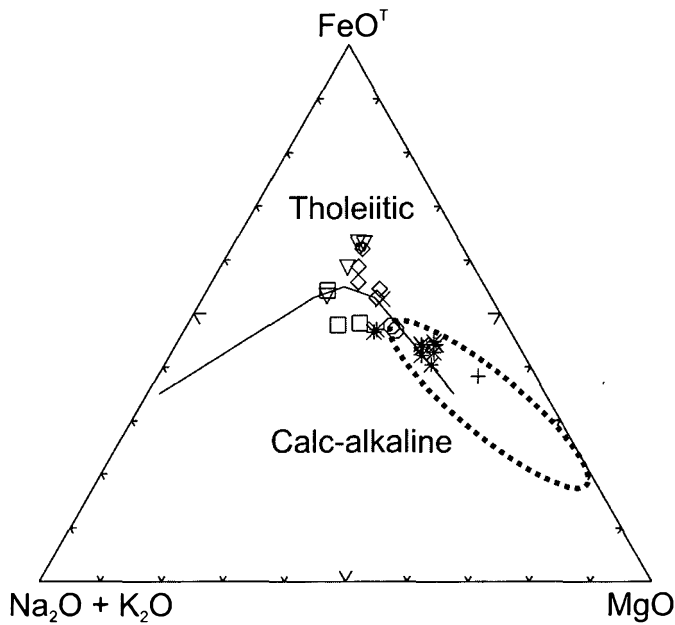
Fig. 7. FeO^T–Na₂O+K₂O–MgO ternary diagram from Irvine and Baragar (1971). Field outlined by dashes includes 15 samples from the St. Stephen Intrusion. Symbols are as in Fig. 4.

REE as well as Nb, Hf, Zr, Ti, and V reflecting a less depleted evolution of the mantle source. The East Branch Brook metagabbro samples have higher V than the Bocabec and St. Stephen samples (Fig. 11b). The St. Stephen Intrusion displays a spider plot significantly different from those of the other two intrusions and tends to more closely resemble that of E-MORB.

SM-ND ISOTOPES

Samples from each of the three types of the EBB metagabbro were sent to Activation Laboratories (Ancaster, Ontario) for Nd isotope analysis by TIMS (Thermal Ionization

Mass Spectrometry). Errors associated with this method as well as the analytical and calculated data for the three types of EBB metagabbro samples are given in Table 3. Based on an approximated age of 410 Ma, the calculated ε_{Nd} for KM-00-22 (type 3), KM-00-24 (type 2), and KM-00-158 (type 1) are 1.08, 2.22, and 3.68 respectively. The positive epsilon values indicate that these metagabbroic dykes were derived from a source depleted in light REE (i.e. depleted mantle), although their epsilon values do not correspond to that of the depleted mantle at that time.

Sm-Nd analysis of a gabbronorite sample from the Bocabec intrusive complex (Whalen et al. 1994) yielded a $^{143}Nd/^{144}Nd$ value of 0.512806 and a $^{147}Sm/^{144}Nd$ value of 0.1602. These values are reasonably close to the type 1 EBB metagabbro. The ε_{Nd} calculated for 410 Ma using the data obtained from Whalen et al. (1994) yielded a slightly lower value (+3.30) than that of the type 1 EBB metagabbro sample.

DISCUSSION

The region hosting the EBB metagabbroic dykes has had a complex tectonic history as several tectonostratigraphic terranes were juxtaposed during subduction and strike-slip faulting (Barr and White 1996; van Staal et al. 1998). A tectonic model recently proposed by Fyffe et al. (1999) to explain the evolution of the area provides a basis upon which to construct a genetic model for the EBB metagabbroic dykes. In this model, a major suture zone is recognized as lying somewhere in the vicinity of the Rollingdam area (e.g., Fyffe et al. 1999) that is, in part, represented by the Sawyer Brook Fault, which separates the St. Croix terrane of the Gander Zone from the peri-Gondwanan New River terrane. Closure of small marginal basins along the southeastern periphery of the Iapetus Ocean caused the collision of the peri-Gondwanan terranes (that include the New River, Brookville, and Caledonia terranes) with the Gander Zone terranes (Fyffe et al. 1999). The interpreted timing of the collision between the
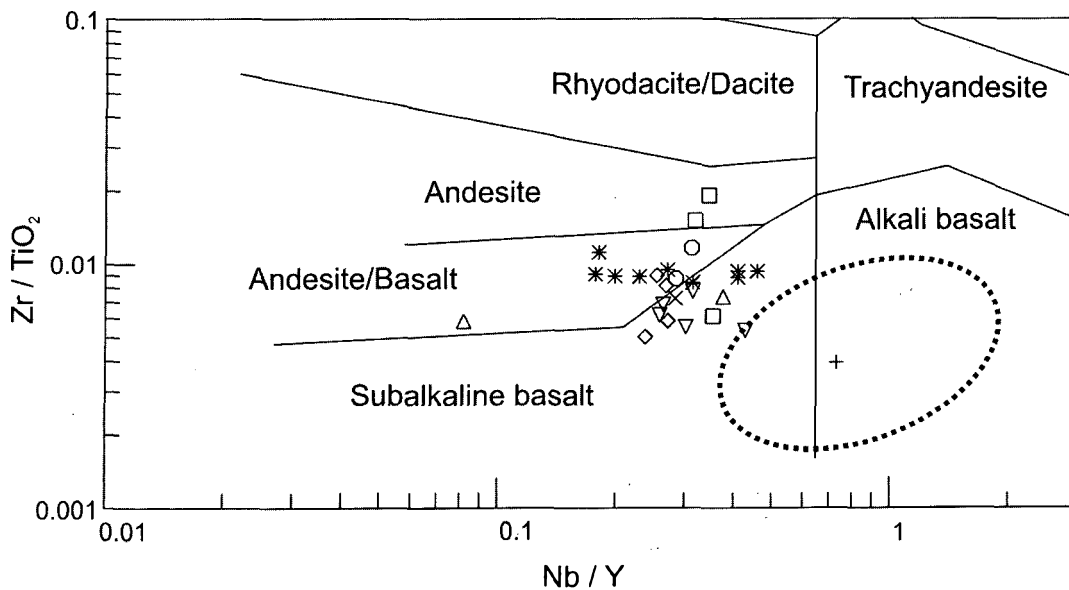
Fig. 8. Nb/Y versus Zr/TiO₂ compositional discrimination diagram from Winchester and Floyd (1977). Field outlined taken from the St. Stephen Intrusion (Paktunc 1989). Symbols are as in Fig. 4.

Table 3. Sm-Nd isotopic data for the three types of East Branch Brook metagabbroic dykes.

Sample	Type	Sm	Nd	$\frac{^{147}Sm}{^{144}Nd}$	$\frac{^{143}Nd}{^{144}Nd_{present}}$	$\varepsilon Nd_{present}$	Age (Ma)	$\frac{^{143}Nd}{^{144}Nd_{initial}}$	CHUR (T)	$\varepsilon Nd(T)$
22	3	7.8	20	0.23485	0.512796	3.08	410	0.512165	0.512110	1.08
24	2	6.8	19	0.21552	0.512802	3.20	410	0.512223	0.512110	2.22
158	1	4.2	16	0.15808	0.512723	1.66	410	0.512299	0.512110	3.68
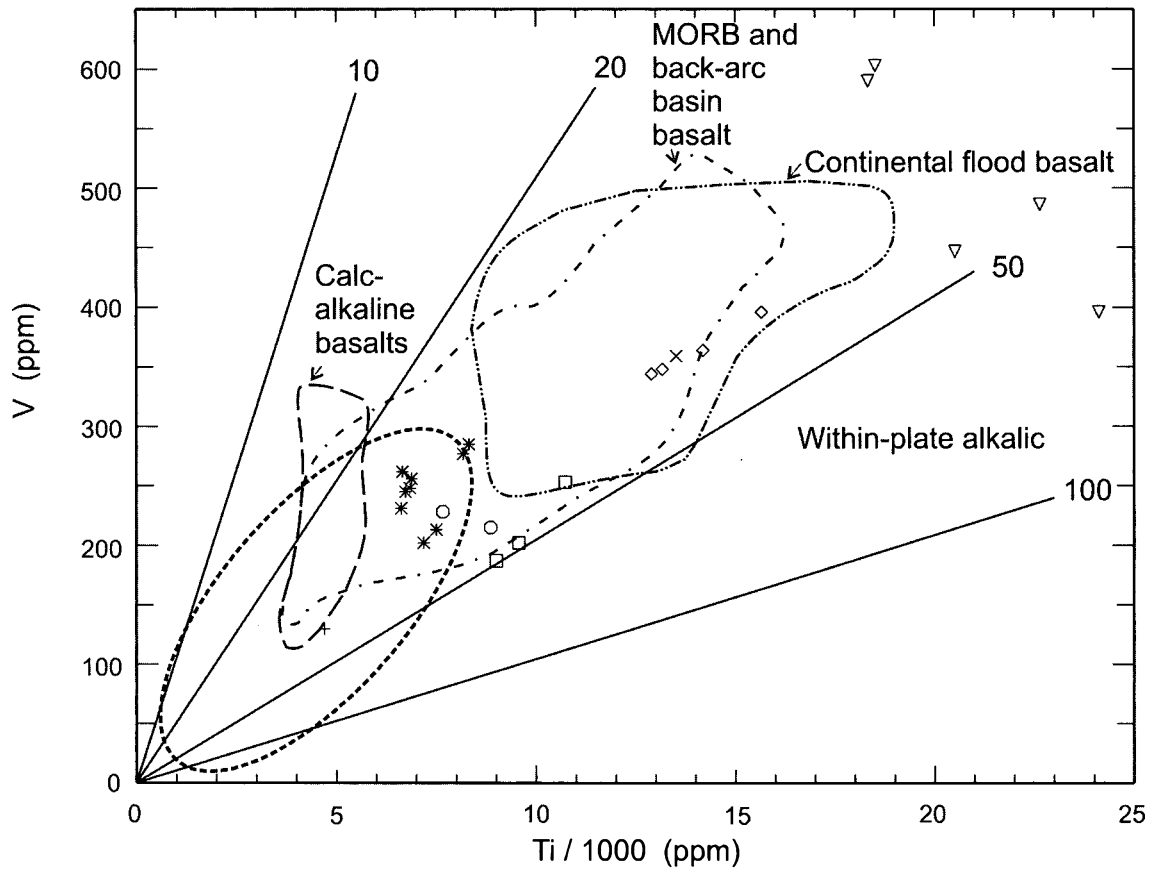
Fig. 9. Ti versus V geochemical discrimination plot (Shervais 1982) with approximated tectonic fields. Dotted field represents 15 samples from the St. Stephen Intrusion (Paktunc 1989). Symbols are as in Fig. 4.

AI: Within-plate alkali basalt
AII: Within-plate alkali basalt
    Within-plate tholeiite
B: Enriched MORB
C: Within-plate tholeiite
    Volcanic-arc basalt
D: Normal MORB
    Volcanic-arc basalt
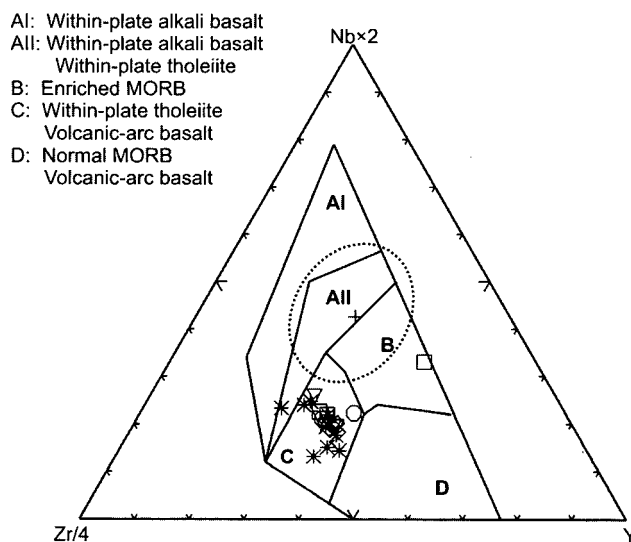
Fig. 10. Zr-Nb-Y mafic geotectonic environment discrimination diagram (Meschede 1986). St. Stephen Intrusion samples represented by the outlined field. Symbols are as in Fig. 4.
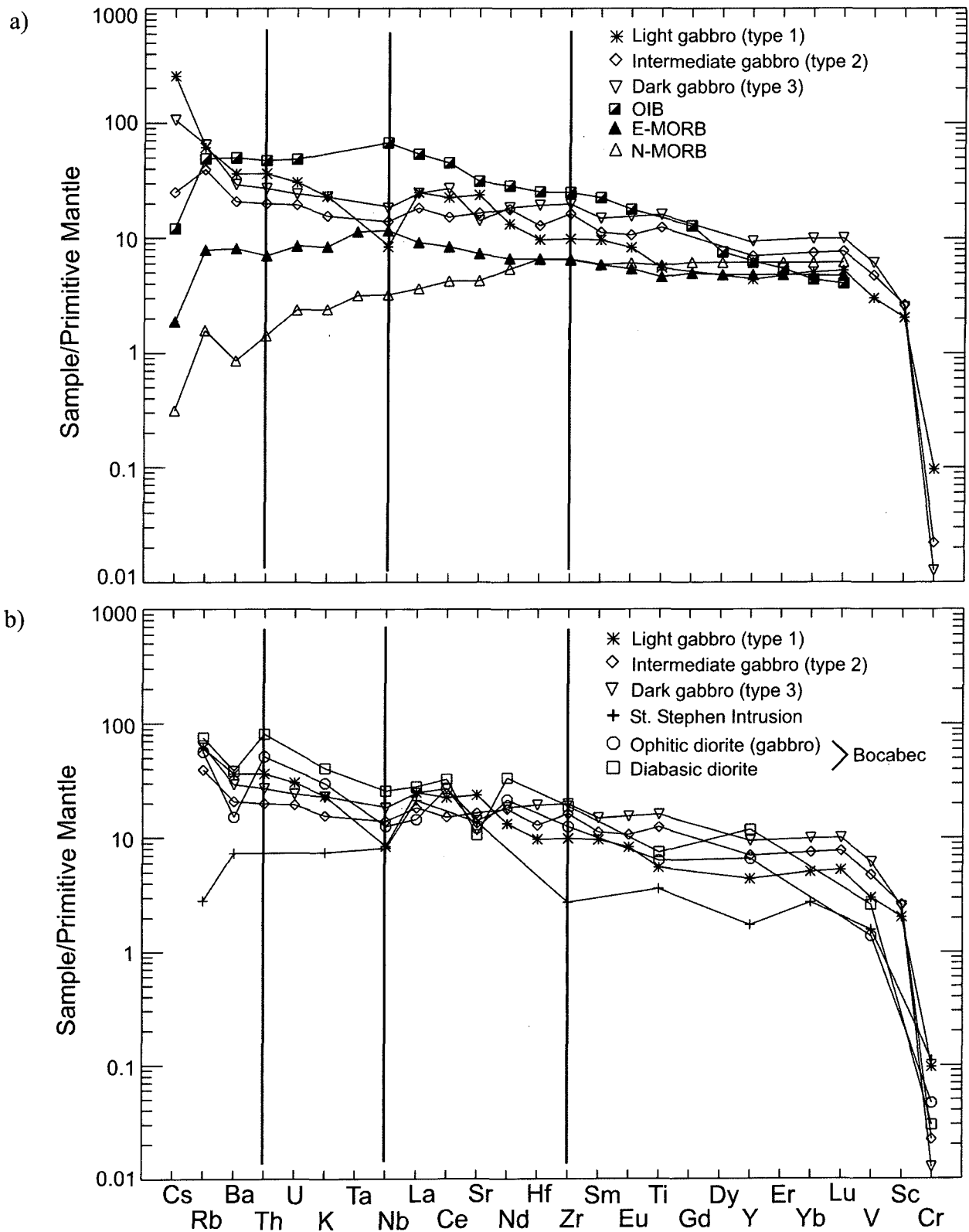
Fig. 11. Modified primitive-mantle normalized spider diagram for the (a) East Branch Brook metagabbroic samples with N-MORB, E-MORB and OIB, and (b) the East Branch Brook metagabbroic samples with data from the Bocabec and St. Stephen (Paktunc 1989) intrusions. Primitive mantle normalizing values are from Sun and McDonough (1989).

New River and St. Croix terranes is Late Ordovician (Fyffe *et al.* 1999) with deposition of Silurian cover sequences occurring soon after, which obscures the boundary and provides an upper constraint on the time of amalgamation. To the north of the Rollingdam area, Early Silurian deep-water sediments of the Digdeguash Formation were deposited in the Fredericton Trough. To the south, shallow marine sedimentary rocks of the Oak Bay and Waweig formations were deposited during development of the Mascarene back-arc basin and Kingston arc. Timing of accretion of the Brookville terrane and synchronous development of the Kingston arc on the southeastern margin of the New River terrane is not well constrained but is interpreted to have taken place during Silurian time (Barr and White 1996; Fyffe *et al.* 1999). Oblique collision occurred between the Brookville and Caledonia terranes during Late Silurian to Early Devonian time (Fyffe *et al.* 1999). Compressional forces on the Mascarene Basin subsequent to Silurian–Devonian sedimentation caused reactivation of northeast-trending faults, which were intruded during the Late Silurian to Early Devonian by both mafic and felsic intrusions (Fyffe *et al.* 1999). If rifting did occur in the Rollingdam area during the Silurian in response to extensional tectonics as suggested by Fyffe *et al.* (1999), it is possible that the crustal scale faults tapped the mantle and provided a focus for the ascent of EBB mafic magmas. This model is consistent with their geochemical signature and would also explain their discordant relationship with the surrounding strata.

A preliminary review of the geochemical data obtained from analyses of the EBB metagabbro intrusions and Bocabec intrusive complex and from previously published analytical data from the St. Stephen intrusion (Paktunc 1989) suggests that these mafic intrusions are not the same. That is, the subalkaline tholeiitic EBB dykes have geochemical attributes consistent with emplacement in a rift in continental crust, whereas the Bocabec diorite has a calc-alkaline signature (based on major element geochemistry; Fig. 7), generally considered typical of a destructive plate margin. The geochemistry of the St. Stephen intrusion reflects a dominantly tholeiitic affinity, although the geochemical composition is quite different from those of the EBB and Bocabec intrusions.

Despite this overview of contrasting geochemical signatures among the intrusions (East Branch Brook, Bocabec, and St. Stephen), geochemical similarities exist between the type 1 EBB metagabbroic dykes and the ophitic diorite (gabbro) of the Bocabec intrusive complex. This similarity may be explained in terms of a common magmatic source for both of the intrusions while the subsequent pulses of magmatism (type 2 and type 3) were most likely from a less depleted source and were emplaced during fault reactivation.

It must be kept in mind that each of the discrimination diagrams used to determine the tectonic settings of magmas have potential errors associated with them, as discussed by Wang and Glover (1992). Conclusions drawn from these discrimination plots concerning tectonic activity can be ambiguous. For example, the Shervais (1982) plot (Fig. 9) is designed for undifferentiated extrusive rocks and the fact that the samples used in this study are intrusive may be an issue in the case of the Bocabec and St. Stephen samples. However,

the gabbro comprising the EBB intrusions is relatively fine grained. This same plot appears to classify the magmas of the EBB metagabbroic samples into three separate environments, fields for which are based solely on empirical data (Wang and Glover 1992) allowing room for error in their classification.

Like the tectonic discrimination diagrams, the spider diagrams produced using data obtained from altered samples can lead to erroneous conclusions on the tectonic setting of the initial magmas. Because the EBB metagabbroic dykes have experienced slight effects of hydrothermal alteration, it is important to incorporate into the spider plots, elements that are considered to be immobile (i.e. Th, Nb, Ta, Zr, Ti and Hf) under most alteration processes (Jenner 1996). Overall, these elements do not exhibit extreme enrichments or depletions with the exception of Nb, which is likely a result of crustal contamination as opposed to alteration.

As the type 1 metagabbro has the highest ε_{Nd} value, it can be concluded that it was derived from a more depleted source than the subsequent type 2 and 3 metagabbro. Because this value does not correspond to that of the depleted mantle, it is assumed that it was contaminated with crustal components or components from the mantle wedge. This conclusion is supported by the negative Nb anomaly already described. The later intrusions with ε_{Nd} values that trend towards CHUR, reflect a more enriched source than the initial phase. This is most likely not a function of crustal contamination, but rather a result of tapping of a deeper mantle source with continued rifting.

It is clear that the gabbroic bodies that exist within the Clarence Stream area created a favourable rheological and chemical environment for gold deposition as these intrusions host disseminated gold in addition to gold-bearing quartz veins. Auriferous quartz veins are better preserved and less deformed in the vicinity of the metagabbroic dykes than those that are hosted by less competent metasedimentary rocks. The igneous bodies tend to shield the quartz veins by taking up the bulk of the strain. Hydrothermal sulphidization of the iron in the metagabbro produced a geochemical trap, which promoted disseminated gold deposition. This explains the greater gold abundances within the alteration selveges of quartz veins hosted within metagabbroic bodies compared to the metasedimentary host rocks.

The tectonic setting of the EBB dykes is similar to that of the mesothermal gold vein-lamprophyre association in the Superior Province of the Canadian Shield where transpressive accretion between terranes or accretion of terranes with a pre-existing continental margin occurred (Kerrich and Wyman 1994). Like the EBB intrusions, these lamprophyres tend to occur as dykes and are proposed to have been generated during low-grade partial melting of a depleted mantle wedge subsequent to collision and uplift (Kerrich and Wyman 1994). Kerrich and Wyman (1994) proposed that the gold deposits are also formed subsequent to collision when rebounding isotherms focused mineralizing fluids up the terrane boundary structures to the mid-crustal level where gold deposition took place. Although evidence suggests that at least one gold mineralizing event responsible for the generation of the Clarence Stream gold deposit was related to the intrusion of the nearby highly evolved phase of the Magaguadavic Granite (Thorne *et al.* 2002), earlier episodes of gold mineralization

may be related to post-collision geodynamics with increased heat flow (similar to those described by Kerrich and Wyman 1994) within the deep-rooted, terrane-bounding fault system that is, in part, occupied by the EBB metagabbroic dykes.

CONCLUSIONS

The East Branch Brook metagabbroic dykes host the Clarence Stream gold deposit in combination with Silurian volcaniclastic sedimentary rocks of the Waweig Formation. The dykes intrude along pre-existing structures that were later reactivated during a gold mineralizing event. Geochemical analyses indicate that these dykes have a tholeiitic signature characteristic of a continental rift environment. They exhibit spider diagram patterns similar to those of the Bocabec intrusive complex, although major-element discrimination plots indicate that the latter has an arc-like signature. Back-arc rifting in an extensional or transtensional setting is interpreted to have occurred in the Silurian (Fyffe et al. 1999) and may have led to the generation of multiple types of the EBB dykes [i.e. light, Mg-rich (type 1); medium (type 2); and dark, Fe-rich (type 3)] with type 1 possibly containing greater proportions of assimilated material than the later type 2 and 3 dykes. Such a genetic model can also explain their discordant relationship with the surrounding strata. The EBB intrusions may have been emplaced along steep terrane-bounding faults during ascent of mantle-derived magmas.

Geochemical signatures of the three types of EBB dykes in conjunction with Sm-Nd isotope data indicate that the initial subalkaline mafic magmas were derived from a depleted mantle (supra subduction) source (positive ε_{Nd} value) and were possibly contaminated with crustal material (LIL element enrichment; Nb depletion). Subsequent intrusions were most likely derived from separate reservoirs of partially depleted mantle sources and the type 3 metagabbro, which exhibits a REE signature resembling OIB (upwelling asthenospheric mantle), is geochemically the closest of the three types to CHUR. These later dykes also exhibit less evidence of contamination, consistent with their injection into the same terrane-bounding fault that was previously intruded by the earliest (type 1) gabbro.

The EBB metagabbroic suite appears to have provided favourable rheological conditions to focus gold mineralization in areas of high strain. The brittle to ductile shear zones that are occupied by the dykes were most likely originally formed in response to local transpressional tectonics that provided conduits for magmas and subsequent mineralizing fluids. This tectonic environment (i.e. terrane accretion) is similar to that described for mesothermal shear zone hosted gold deposits that also commonly focus lamprophyre dykes (Kerrich and Wyman 1994).

Determining the age of these mafic intrusions will be particularly useful in defining a genetic model for the gold mineralizing event. The earliest mineralization is no older than Silurian because the EBB intrusions host disseminated gold and gold-bearing quartz veins that appear to be discordant to Silurian strata of the Waweig Formation. Their upper age limit is constrained by cross-cutting pegmatite and aplite dykes that have been dated at 390 ± 8 Ma (Thorne et al. 2002).

REFERENCES

BARR, S.M., & WHITE, C.E. 1996. Contrast in late Precambrian-early Paleozoic tectonothermal history between Avalon composite terrane sensu stricto and other possible peri-Gondwanan terranes in southern New Brunswick and Cape Breton Island, Canada. In Avalonian and Related Peri-Gondwanan Terranes of the Circum-North Atlantic. Edited by R.D. Nance and M.D. Thompson. Geological Society of America, Special Paper 304, pp. 95–108.

BEVIER, M.L. 1990. Preliminary U-Pb geochronologic results for igneous and metamorphic rocks, New Brunswick. In Project Summaries for 1989, Fourteenth Annual Review of Activities. Edited by S. A. Abbott. New Brunswick Department of Natural Resources and Energy Division, Information Circular 89–2 (Second Edition), pp. 208–212.

CHERRY, M.E. 1976. The petrogenesis of granites in the St. George Batholith, southwestern New Brunswick, Canada. Ph. D. thesis, University of New Brunswick, New Brunswick, 242 p.

COX, K.G., BELL, J.D., & PANKJURST, R.J. 1979. The Interpretation of Igneous Rocks. George, Allen, and Unwin, London.

FYFFE, L.R. 1971. Petrogenesis of the adamellite-diorite transition, southwestern New Brunswick. Unpublished M. Sc. Thesis, University of New Brunswick, 130 p.

FYFFE, L.R., & FRICKER, A. 1987. Tectonostratigraphic terrane analysis of New Brunswick. Maritime Sediments and Atlantic Geology, 23, pp. 113–122.

FYFFE, L.R., & RIVA, J. 1990. Revised stratigraphy of the Cookson Group of southwestern New Brunswick and adjacent Maine. Atlantic Geology, 26, pp. 271–275.

FYFFE, L.R., PICKERILL, R.K., & STRINGER, P. 1999. Stratigraphy, sedimentology and structure of the Oak Bay and Waweig formations, Mascarene Basin: implications for the evolution of southwestern New Brunswick. Atlantic Geology, 35, pp. 59–84.

GRAHAM, C.M. 1976. Petrochemistry and tectonic significance of Dalradian metabasaltic rocks of S.W. Scottish Highlands. Journal of Geological Society, London, 132, pp. 61–84.

HOY, D. 2001. Assessment report for the Clarence Stream gold deposit, southwestern New Brunswick. New Brunswick Department of Natural Resources and Energy, Assessment File.

IRVINE, T.N., & BARAGAR, W.R.A. 1971. A guide to the chemical classification of the common volcanic rocks. Canadian Journal of Earth Sciences, 8, pp. 523–548.

JENNER, G.A. 1996. Geochemical nomenclature and analytical chemistry. In Trace Element Geochemistry of Volcanic Rocks: Applications for Massive Sulphide Exploration. Edited by D. A. Wyman. Geological Association of Canada Short Course Notes, 12, pp. 51–78.

JOHNSON, S.D., & McLEOD, M.J. 1996. The New River Belt: A unique segment along the western margin of the Avalon composite terrane, southern New Brunswick, Canada. *In* Avalonian and Related Peri-Gondwanan Terranes of the Circum-North Atlantic. *Edited by* R.D. Nance and M. D. Thompson. Geological Society of America Special Paper 302, pp. 149–164.

KERRICH, R., & WYMAN, D.A. 1994. The mesothermal gold-lamprophyre association: significance for an accretionary geodynamic setting, supercontinent cycles, and metallogenic processes. Mineralogy and Petrology, 51, pp. 147–172.

LENTZ, D.R. 1995. Preliminary evaluation of six in-house rock geochemical standards from the Bathurst Camp, New Brunswick. *In* Current Research 1994. *Compiled and Edited by* S.A.A. Merlini. New Brunswick Department of Natural Resources and Energy, Minerals and Energy Division, Miscellaneous Report 18, pp. 81–89.

McLEOD, M.J. 1990. Geology, geochemistry, and related mineral deposits of the Saint George Batholith; Charlotte, Queens, and Kings Counties, New Brunswick. New Brunswick Department of Natural Resources and Energy, Mineral Resources, Mineral Resource Report 5, 169 p.

McLEOD, M.J., JOHNSON, S.C., & FYFFE, L.R. 1998. Bedrock geological compilation of the McDougall Lake area (NTS 21 G/07), Charlotte County, New Brunswick. New Brunswick Department of Natural Resources and Energy, Mines and Energy Division, Plate 98–25.

MESCHEDE, M. 1986. A method of discriminating between different types of mid-ocean ridge basalts and continental tholeiites with the Nb-Zr-Y diagram. Chemical Geology, 56, pp. 207–218.

NEW BRUNSWICK DEPARTMENT OF NATURAL RESOURCES AND ENERGY. 2000. Bedrock geology of New Brunswick, Minerals and Energy Division, Map NR-1 (2000 edition). Scale 1:500 000.

PAKTUNC, A.D. 1986. St. Stephen mafic-ultramafic intrusion and related nickel-copper deposits, New Brunswick. Geological Survey of Canada Paper, 86-1A, pp. 327–331.

PAKTUNC, A.D. 1987. Nickel, copper, platinum and palladium relations in Ni-Cu deposits of the St. Stephen intrusion, New Brunswick. Geological Survey of Canada Paper, 87-1A, pp. 543–553.

PAKTUNC, A.D. 1989. Petrology of the St. Stephen Intrusion and the genesis of related nickel-copper sulphide deposits. Economic Geology, 84, pp. 817–840.

RUITENBERG, A.A., JOHNSON, S.C., & FYFFE, L.R. 1990. Epigenetic gold deposits and their tectonic setting in the New Brunswick Appalachians. CIM Bulletin, 83, No. 934, pp. 43–55.

SHERVAIS, J.W. 1982. Ti-V plots and the petrogenesis of modern and ophiolitic lavas. Earth and Planetary Science Letters, 59, pp. 101–118.

STEPHENS, M.G. 1982. Field relationships, petrochemistry and petrogenesis of the Stekenjokk volcanicites, central Swedish Caledonides. Norges Geologiske Undersøgelse, 360, pp. 159–193.

STILLMAN, C.J., & WILLIAMS, C.T. 1979. Geochemistry and tectonic setting of some Ordovician volcanic rocks in east and southeast Ireland. Earth and Planetary Science Letters, 41, pp. 288–310.

SUN, S.-S., & McDONOUGH, W.F. 1989. Chemical and isotopic systematics of oceanic basalts: implications for mantle composition and processes. *In* Magmatism in the Ocean Basins. *Edited by* A. D. Saunders and M.J. Norry. Geological Survey of Canada Special Publication No. 42, Blackwell Scientific Publications, 398 pp.

THORNE, K.G., & LENTZ, D.R. 2001. Geological setting of the Clarence Stream gold deposit, southwestern New Brunswick. *In* Guidebook to Field Trips in New Brunswick and Eastern Maine. *Edited by* R. Pickerill and D. Lentz. 93rd Annual Meeting, New England Intercollegiate Geological Conference, pp. C5-1-16.

THORNE, K.G., HOY, D., & LENTZ, D.R. 2001. Controls on gold mineralization at the Clarence Stream deposit, northern Saint George Batholith, southwestern New Brunswick. North Atlantic Minerals Symposium, Extended Abstract Volume, pp. 166–168.

THORNE, K.G., LENTZ, D.R., HALL, D.C., & YANG, X. 2002. Petrology, geochemistry, and geochronology of the granitic pegmatitic and aplite dykes associated with the Clarence Stream gold deposit, southwestern New Brunswick. Geological Survey of Canada, Current Research 2002-E12, 13 p.

VAN STAAL, C.R., DEWEY, J.F., MACNIOCAILL, C., & McKERROW, W.S. 1998. The Cambrian-Silurian Appalachians and British Caledonides: history of a complex, west and southwest Pacific-type segment of Iapetus. *In* Lyell; The Past is the Key to the Present. *Edited by* D.J. Blundell and A.C. Scott. Geological Society, London, Special Publication 143, pp. 199–242.

WANG, P., & GLOVER, L., III. 1992. A tectonics test of the most commonly used geochemical discriminant diagrams and patterns. Earth Science Reviews, 33, pp. 111–131.

WANLESS, R.K., STEVENS, R.D., LACHANCE, G.R., & DELABIO, R.N. 1973. K-Ar age determinations of samples from various areas of New Brunswick. *In* Age Determinations and Geological Studies; K-Ar Isotopic Ages. Geological Survey of Canada, Report 11, Paper 73-2, pp. 78–90.

WHALEN, J.B., FYFFE, L.R., LONGSTAFFE, F.J., & JENNER, G.A. 1996. The position and nature of the Gander-Avalon boundary, southern New Brunswick, based on geochemical and isotopic data from granitoid rocks. Canadian Journal of Earth Sciences, 33, pp. 129–139.

WHALEN, J.B., JENNER, G.A., CURRIE, K.L., BARR, S.M., LONGSTAFFE, F.J., & HEGNER, E. 1994. Geochemical and isotopic characteristics of granitoids of the Avalon Zone, southern New Brunswick: possible evidence for repeated delamination events. Journal of Geology, 102, pp. 269–282.

WILSON, M. 1989. Igneous Petrogenesis. Unwin Hyman, London.

WINCHESTER, J.A., & FLOYD, P.A. 1977. Geochemical discrimination of different magma series and their differentiation products using immobile elements. Chemical Geology, 20, pp. 325–343.

Editorial responsibility: Sandra M. Barr

Appendix 1. Analyses of the East Branch Brook and Bocabec Intrusive Complex samples.

Samples	KM18	KM19	KM20	KM21	KM22	KM23	KM24	KM25	KM26	KM113	KM145	KM146
Type	3	1	1	1	3	3	2	1	1	2	3	2
Major elements (wt%)												
SiO_2	49.7	49.6	49.8	49.9	48.2	49.6	47.3	48.9	48.2	48.9	46.9	49.0
TiO_2	4.02	1.14	1.12	1.11	3.78	3.42	4.18	1.25	1.20	2.15	3.09	2.61
Al_2O_3	13.90	15.39	15.22	15.46	13.40	12.42	12.93	17.33	17.88	14.29	14.32	14.21
$Fe_2O_3^T$	11.30	9.89	9.69	10.03	16.18	15.07	16.35	9.96	9.66	13.02	15.16	14.79
MnO	0.22	0.17	0.18	0.22	0.25	0.24	0.26	0.20	0.16	0.22	0.26	0.28
MgO	3.8	8.5	8.7	8.8	5.0	4.8	5.1	8.1	8.1	6.0	4.6	5.1
CaO	8.6	10.93	10.21	9.72	8.43	7.8	8.09	10.55	10.08	9.57	9.93	7.83
Na_2O	4.16	2.31	2.27	2.49	3.45	3.95	3.47	1.99	2.25	3.09	2.75	3.64
K_2O	0.94	0.40	0.69	1.10	0.45	0.84	0.44	1.21	0.37	0.64	0.66	0.61
P_2O_5	0.63	0.18	0.18	0.18	0.50	0.48	0.46	0.16	0.18	0.29	0.29	0.36
LOI	2.2	0.9	1.7	0.8	1.0	1.0	1.3	1.0	1.5	1.3	0.7	1.2
Total	97.3	98.5	98.1	98.9	99.6	98.7	98.5	99.7	98.1	98.2	98.0	98.4
S	0.93	0.01	0.00	0.01	0.22	0.36	0.12	0.08	0.15	0.05	0.86	0.07
Mg#	40.2	63.1	64.1	63.4	37.7	38.7	38.1	61.7	62.4	47.7	37.5	40.5
Trace elements (in ppm, except Au in ppb)												
Pb	35	2	14	7	7	5	11	11	2	7	361	117
Cu	106	8	5	3	38	50	9	24	49	32	119	20
V	396	248	245	262	486	447	503	213	202	344	603	396
Sc	45	38	37	39	49	45	49	32	33	47	39	44
Co	34	34	32	33	39	32	37	39	38	28	45	29
Ni	12	93	105	105	35	26	19	97	65	32	23	25
Cr	41	362	369	387	47	42	38	196	200	76	28	74
Zn	158	81	125	174	132	162	144	149	82	100	121	160
Bi	0.26	0.05	0.16	0.12	0.05	0.23	0.05	0.10	0.05	0.03	0.58	0.49
Cd	1.2	0.7	0.2	0.5	1.4	0.5	1.0	0.5	0.5	0.2	0.2	0.3
In	n.d.	n.d.	n.d.	n.d.	n.d.	n.d.	n.d.	n.d.	n.d.	n.d.	n.d.	0.2
Sn	n.d.	n.d.	n.d.	n.d.	n.d.	n.d.	n.d.	n.d.	n.d.	1	4	1
W	n.d.	n.d.	n.d.	n.d.	n.d.	n.d.	n.d.	n.d.	n.d.	n.d.	n.d.	n.d.
Mo	3	2	1	2	3	3	2	2	3	1	1	1
As	704	373	103	210	57	42	84	168	201	101	440	101
Se	1.0	0.4	0.4	0.4	0.9	0.7	0.6	0.2	0.3	1.5	1.5	1.5
Sb	193	39.3	20	28.7	92.5	11.3	22.7	331	278	2.3	5	1.5
Te	n.d.	n.d.	n.d.	n.d.	n.d.	n.d.	n.d.	n.d.	n.d.	0.1	0.1	0.1
Nb	18	6	4	7	13	13	11	7	6	9	12	9
Ta	n.d.	n.d.	n.d.	n.d.	1.00	1.00	n.d.	n.d.	n.d.	n.d.	n.d.	n.d.
Li	–	–	–	–	–	–	–	–	–	43	11	27
Ga	20	17	16	17	22	17	21	17	17	21	21	21
Tl	n.d.	0.10	n.d.	0.70	0.10	n.d.	n.d.	0.70	n.d.	0.39	0.45	0.42
Sr	368	507	514	440	281	320	340	319	316	328	260	410
Ba	220	250	340	470	210	440	350	85	25	113	76	187
Cs	4	8	6	32	4	2	2	7	13	1	3	1
Rb	51	20	39	84	19	35	20	82	24	38	73	39
Au	253	60	225	87	n.d.	11	3	n.d.	46	n.d.	2	7
Ag	n.d.	n.d.	n.d.	n.d.	n.d.	n.d.	n.d.	n.d.	n.d.	n.d.	n.d.	n.d.
Zr	310	106	100	103	232	233	210	110	113	165	164	152
Y	57	13	20	17	50	49	46	17	22	36	28	33
La	23.9	15.7	18.9	15.8	20.0	18.1	17.3	9.9	9.8	11.7	12.0	9.5
Th	3.8	3.6	3.5	3.5	2.3	2.8	2.5	1.6	1.6	1.2	1.2	1.6
U	n.d.	n.d.	1.20	n.d.	n.d.	1.20	n.d.	n.d.	n.d.	0.40	0.70	0.40
Ce	59	37	40	39	50	45	46	26	27	23	44	29
Pr	–	–	–	–	–	–	–	–	–	5.4	5.5	5.2
Nd	28	19	22	12	20	27	19	10	6	27	17	18
Sm	9.1	4.5	4.3	4.4	7.8	7.5	6.8	3.7	3.5	4.4	4.7	4.9
Eu	3.9	1.6	1.5	1.5	2.9	2.8	2.9	1.4	1.3	1.6	1.8	1.7
Gd	–	–	–	–	–	–	–	–	–	5.1	5.1	5.3
Tb	1.60	0.70	0.60	n.d.	1.20	2.00	2.10	n.d.	n.d.	0.80	n.d.	0.90
Dy	–	–	–	–	–	–	–	–	–	5.7	5.5	5.6
Ho	–	–	–	–	–	–	–	–	–	1.2	1.3	1.3
Er	–	–	–	–	–	–	–	–	–	3.3	3.1	2.9
Tm	–	–	–	–	–	–	–	–	–	0.5	0.5	0.5
Yb	6.9	2.9	2.7	2.9	5.4	5.7	5.1	2.8	2.7	3.1	3.3	3.5
Lu	1.05	0.45	0.41	0.44	0.81	0.85	0.77	0.42	0.41	0.46	0.50	0.53
Br	n.d.	n.d.	n.d.	n.d.	n.d.	n.d.	n.d.	n.d.	n.d.	n.d.	n.d.	n.d.
Be	1.0	n.d.	n.d.	n.d.	1.0	2.0	2.0	n.d.	n.d.	1.0	2.0	1.3
Hf	8	3	2	3	6	6	6	3	3	2	4	4

Notes: Types 1 (light), 2 (intermediate) and 3 (dark); * samples from Fyffe (1971); n.d. = below detection limit.

Appendix 1 (contd.)

Samples	KM150	KM155	KM156	KM157	KM158	KM159	KM160	F25*	560*	563*	753*	754*
Type	3	2	1	2	1	1	1					
Major elements (wt%)												
SiO_2	46.8	51.2	48.9	50.6	49.6	49.5	48.1	49.1	53.2	55.3	54.6	48.9
TiO_2	3.06	2.2	1.15	2.37	1.39	1.37	1.11	1.48	1.6	1.5	1.79	1.28
Al_2O_3	15.17	14.12	15.36	14.00	16.90	16.46	14.72	16.66	15.35	14.86	14.18	16.55
$Fe_2O_3^T$	15.40	11.40	10.44	13.48	10.75	11.18	10.18	10.32	10.08	9.53	11.63	10.89
MnO	0.23	0.18	0.22	0.23	0.18	0.17	0.17	0.17	0.20	0.20	0.24	0.16
MgO	4.4	5.5	8.7	5.2	6.5	6.7	9.8	6.8	5.3	4.4	3.8	6.9
CaO	9.5	10.35	9.46	7.95	7.63	7.68	8.89	9.53	7.48	6.68	7.16	9.42
Na_2O	3.09	3.38	2.87	3.99	4.13	4.06	2.66	3.01	3.54	3.55	3.66	2.80
K_2O	0.58	0.25	0.51	0.41	0.51	0.57	0.97	0.70	0.94	1.38	1.35	1.09
P_2O_5	0.32	0.28	0.18	0.32	0.22	0.22	0.27	0.24	0.27	0.26	0.30	0.15
LOI	1.1	0.8	1.4	0.8	1.7	2.1	2.2	–	–	–	–	–
Total	98.6	98.8	97.8	98.6	97.8	97.9	96.9	98.1	97.9	97.7	98.7	98.1
S	1.50	1.50	1.50	1.50	1.50	1.50	1.50	–	–	–	–	–
Mg#	36.2	48.9	62.2	43.3	54.3	54.2	65.7	56.8	50.8	47.7	39.2	55.5
Trace elements (in ppm, except Au in ppb)												
Pb	162	108	113	67	6	15	0	4	2	11	–	–
Cu	27	15	67	22	51	12	23	–	–	–	–	–
V	590	348	256	364	285	277	231	215	202	187	253	228
Sc	39	44	36	41	33	35	33	–	–	–	–	–
Co	20	13	33	20	37	40	45	46	31	41	54	57
Ni	16	20	96	19	50	44	166	101	66	48	17	69
Cr	29	80	356	59	126	121	440	150	128	97	36	122
Zn	92	88	142	103	95	86	75	104	126	167	116	105
Bi	0.07	0.32	0.03	0.08	0.01	0.01	0.11	–	–	–	–	–
Cd	0.2	0.1	0.2	0.2	0.3	0.2	0.1	–	–	–	–	–
In	0.1	0.1	0.1	0.1	0.1	0.1	0.1	–	–	–	–	–
Sn	1	2	1	1	1	1	1	–	–	–	–	–
W	n.d.	n.d.	n.d.	n.d.	n.d.	n.d.	n.d.	–	–	–	–	–
Mo	137	104	94	56	8	11	2	–	–	–	–	–
As	5	2	7	5	9	12	0	–	–	–	–	–
Se	0.1	0.1	0.1	0.1	0.1	0.1	0.1	–	–	–	–	–
Sb	5.2	2.4	7.4	5.4	8.8	12.2	0.05	–	–	–	–	–
Te	0.1	0.1	0.1	0.1	0.1	0.1	0.1	–	–	–	–	–
Nb	10	10	6	11	5	6	4	10	15	18	22	8
Ta	n.d.	n.d.	n.d.	n.d.	n.d.	1.70	n.d.	–	–	–	–	–
Li	16	6	43	20	44	69	59	–	–	–	–	–
Ga	23	18	15	18	17	15	13	17	19	18	18	16
Tl	0.31	0.06	0.24	0.23	n.d.	0.09	0.76	–	–	–	–	–
Sr	269	294	247	372	710	476	973	274	233	230	213	239
Ba	77	25	270	167	147	253	457	106	226	296	284	108
Cs	4	1	1	1	1	4	3	–	–	–	–	–
Rb	29	8	19	18	9	14	64	19	42	53	48	52
Au	n.d.	n.d.	n.d.	n.d.	n.d.	n.d.	n.d.	–	–	–	–	–
Ag	n.d.	n.d.	n.d.	n.d.	n.d.	n.d.	n.d.	–	–	–	–	–
Zr	168	178	96	212	126	121	123	171	240	286	109	111
Y	33	37	19	43	28	26	22	32	47	52	62	28
La	10.6	11.8	13.9	12.7	16.7	17.4	36.1	20.0	19.0	20.0	19.0	–
Th	1.2	1.4	2.9	1.8	3.3	3.4	4.6	5.7	6.3	6.4	8.1	3.1
U	0.30	0.30	0.90	0.70	0.70	0.80	1.20	–	–	–	–	–
Ce	42	27	51	35	14	61	61	66	44	50	81	29
Pr	4.9	5.6	5.5	6.2	6.5	6.9	12.4	–	–	–	–	–
Nd	32	24	11	30	16	30	27	34	29	50	57	24
Sm	4.0	4.2	3.9	4.7	4.2	4.3	4.2	–	–	–	–	–
Eu	1.5	1.5	1.2	1.4	1.4	1.2	1.9	–	–	–	–	–
Gd	5.0	5.5	3.6	5.9	5.0	4.2	5.0	–	–	–	–	–
Tb	n.d.	1.00	0.70	1.00	1.00	n.d.	0.90	–	–	–	–	–
Dy	5.4	5.7	3.4	6.4	4.0	3.9	3.6	–	–	–	–	–
Ho	1.2	1.3	0.8	1.5	0.9	0.8	0.8	–	–	–	–	–
Er	2.9	3.3	1.9	3.6	2.1	2.2	1.9	–	–	–	–	–
Tm	0.4	0.5	0.3	0.5	0.3	0.3	0.3	–	–	–	–	–
Yb	3.2	3.3	2.2	3.7	2.3	2.3	1.9	–	–	–	–	–
Lu	0.47	0.50	0.35	0.58	0.35	0.35	0.30	–	–	–	–	–
Br	n.d.	n.d.	n.d.	n.d.	n.d.	n.d.	n.d.	–	–	–	–	–
Be	0.9	1.3	0.8	1.1	0.8	0.6	1.1	–	–	–	–	–
Hf	4	5	3	5	4	4	3	–	–	–	–	–